

## Specific Features in the Change of Electrical Resistivity of Carbon Nanocomposites Based on Nanodiamonds under Neutron Irradiation

S. K. Gordeev<sup>a</sup>, R. F. Konopleva<sup>b,\*</sup>, V. A. Chekanov<sup>b</sup>, S. B. Korchagina<sup>a</sup>, S. P. Belyaev<sup>b,d</sup>,  
I. V. Golosovskii<sup>b</sup>, I. A. Denisov<sup>c</sup>, and P. I. Belobrov<sup>c</sup>

<sup>a</sup> Central Research Institute for Materials, ul. Paradnaya 8, St. Petersburg, 191014 Russia

\* e-mail: krf@pnpi.spb.ru

<sup>b</sup> Konstantinov Petersburg Nuclear Physics Institute, National Research Centre “Kurchatov Institute,”  
Orlova Roshcha, Gatchina, Leningrad oblast, 188300 Russia

<sup>c</sup> Siberian Federal University, Institute of Biophysics, Siberian Branch of the Russian Academy of Sciences,  
Akademgorodok 50–50, Krasnoyarsk, 660036 Russia

<sup>d</sup> St. Petersburg State University, Universitetskaya nab. 7–9, St. Petersburg, 199034 Russia

Received November 1, 2012; in final form, December 25, 2012

**Abstract**—The physical properties of bulk composite materials consisting of nanodiamond, pyrolytic carbon, and nanopores were investigated. Samples were irradiated in a channel of the reactor by fast neutrons ( $E > 0.5$  MeV) in ampoules with helium and in an aqueous medium. The dependences of the electrical transport properties of materials with different compositions on the dose of irradiation with fast neutrons were studied. A nonmonotonic change in the electrical resistivity with an increase in the neutron fluence was revealed. Possible explanations were offered for the observed dependence of the electrical resistivity on the neutron fluence, in particular, those related to the physical processes occurring in surface states of the three-phase system of the nanocomposite.

**DOI:** 10.1134/S1063783413070147

### 1. INTRODUCTION

As is known, nanodiamonds were obtained for the first time in Russia by means of the detonation synthesis from molecules of explosives [1]. Nanodiamonds are very small three-dimensionally ordered particles with an average size of 4–5 nm and represent a unique carbon nanoform built up of atoms in the state of  $sp^3$  hybridization.

In this work, the objects of investigation were samples of the composite carbon material based on nanodiamonds. Using the synthetic method, individual particles in a powder nanodiamond preform were bound by pyrolytic carbon. Pyrolytic carbon was prepared by the heterogeneous chemical reaction of decomposition of methane on the entire internal surface of the preform. The synthesis resulted in the for-

mation of a carbon composite material, in which individual nanodiamond particles are bound by pyrolytic carbon [2]. Moreover, the composite is characterized by a high open porosity. This composite material was called NDC. The pyrolytic carbon matrix has a specific graphite-like structure, because the majority of its constituent atoms are in the  $sp^2$ -hybridized state. The average thickness of the pyrolytic carbon layer coating the diamond particles is very small and does not exceed 1 nm. The method used for synthesizing the NDC composite makes it possible to significantly (from 0 to 80%) vary the content of the graphite-like phase and, hence, its average thickness, which is calculated as the ratio of the volume content of pyrolytic carbon to the surface area of pores (see table).

Thus, in the NDC composite, there are three types of interrelated compatible nanofragments, namely,

Composition of the studied samples

NDC type	Content of pyrolytic carbon, %	Porosity of the material, %	Content of nanodiamond, %	Average thickness of the pyrolytic carbon layer, Å
NDC10	5	67	28	2
NDC30	15	57	28	6
NDC40	20	52	28	8

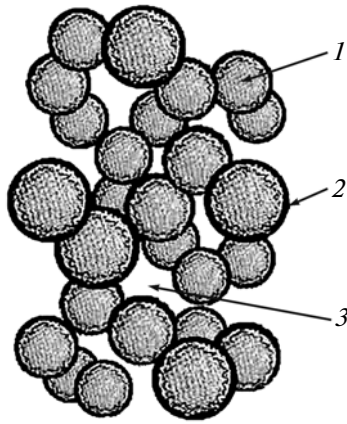


**Fig. 1.** Structure of the diamond–pyrolytic carbon nanocomposite: (1) nanodiamonds with a diameter of 4–5 nm, (2) pyrolytic carbon layer with a thickness of 1 nm, and (3) nanopores with a characteristic size of 8–10 nm.

nanodiamonds, a nanoscale graphite-like matrix (pyrolytic carbon), and nanopores (Fig. 1). On the macroscale, all three phases form a single composite that has a sufficient strength to maintain a specified three-dimensional shape. A large ratio of the surface area to the volume of the material determines a decisive role of the surface in contact phenomena and electrical transport processes occurring in the composite. As was shown in [2, 3], the temperature dependence of the electrical conductivity of NDC composites has a semiconductor character: with an increase in the temperature, the electrical conductivity increases. Moreover, an analysis revealed that, in the NDC composite, the conduction occurs according to the hopping mechanism. This obviously indicates that charge transfer proceeds through the nanodiamond subsystem. At the same time, the electrical conductivity of the NDC composite at the liquid-nitrogen boiling temperature changes by more than 9 orders of magnitude with an increase in the pyrolytic carbon content from 5 to 20%, which suggests a determining role of the pyrolytic carbon matrix in the formation of the electrophysical properties of the material [2, 3].

From the foregoing, it follows that the NDC nanocomposites are very interesting objects of study. The investigation of the mechanisms responsible for the formation of properties of nanostructured composites is an important and urgent problem in the physics of condensed matter. Of particular interest is the possibility of modifying the electrophysical properties of the composites due to exposure of an electrically conductive graphite-like matrix to irradiation with high-energy particles, for example, fast neutrons. It might be expected that the electronic properties of the NDC composite can be controllably modified by means of the generation of radiation defects and transformation of the structure of the nanodiamonds and the graphite-like matrix.

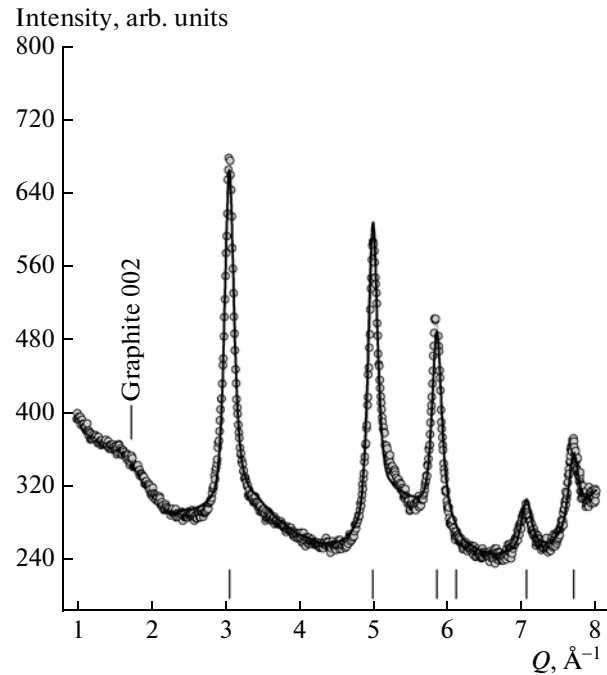


**Fig. 2.** Neutron diffraction pattern of the NDC30 sample. Dashes show positions of the diffraction reflections. The neutron wavelength is 1.38 Å.

The purpose of this work was to investigate the effect of fast neutron irradiation on the electrophysical properties of the carbon nanocomposites NDC.

## 2. EXPERIMENTAL RESULTS

We studied the samples NDC10, NDC30, and NDC40 with contents of the components presented in the table. For the purpose of the structural characterization, we performed neutron diffraction investigations of the NDC30 composition, which is intermediate between the compositions NDC10 and NDC40. Experiments were carried out on a multi-counter neutron diffractometer at the Konstantinov Petersburg Nuclear Physics Institute. The neutron diffraction pattern of the NDC30 sample shown in Fig. 2 exhibits a highly diffuse reflection 002 from a graphite-like (pyrolytic carbon) layer formed in the composite on the surface of nanodiamond particles. A large broadening of this diffraction reflection implies a very small characteristic size, which corresponds to the model of the composite shown in Fig. 1.

The measured neutron diffraction pattern (Fig. 2) contains reflections corresponding to the structure of cubic diamond with the unit cell size of 3.5570(5) Å, which is slightly less than that of diamond single crystals (3.5668 Å). According to the calculation in the isotropic approximation, the average diffraction size of diamond nanoparticles is equal to 3.1(1) nm. The shape of diffraction reflections from diamond nano-

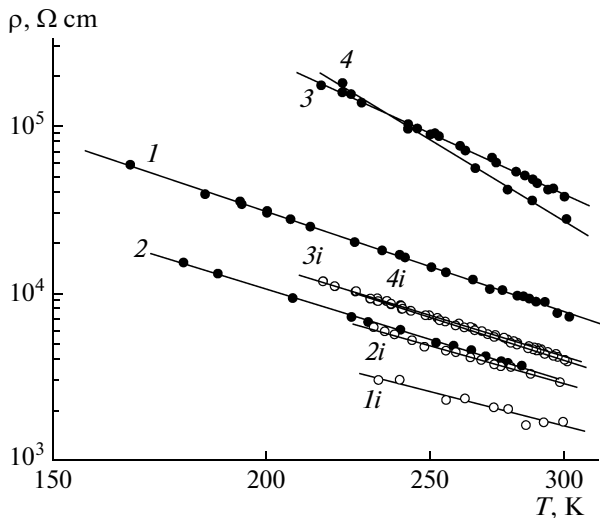


**Fig. 3.** Temperature dependences of the electrical resistivity of (1–4) the NDC10.1 samples irradiated with fluences  $F = (1) 5 \times 10^{16}$ , (2)  $1 \times 10^{17}$ , (3)  $5 \times 10^{17}$ , and (4)  $5 \times 10^{18} \text{ cm}^{-2}$  and (1i–4i) the same samples before irradiation.

particles is not described by a Gaussian profile: in the neutron diffraction pattern (Fig. 2), there is a characteristic “tail” on the right, which is typical of diffraction from quasi-two-dimensional objects [4]. This feature of the neutron diffraction can be explained by the difference in the structures of the surface layer of a diamond nanoparticle and its core. It should be emphasized that this thin surface layer has a crystal structure of diamond and is not graphite-like.

The electrical resistivity of the samples was measured by the four-probe method in the temperature range 77–400 K. For high-resistance samples, the absence of rectification in contacts was controlled by measuring the current–voltage characteristic. To stabilize the resistivity, all samples were preliminarily annealed at a temperature of 500°C for 30 min in argon. Nonetheless, the initial samples had a spread in the resistivity.

The temperature dependences of the electrical resistivity of the NDC10.1 samples unirradiated and irradiated in an aqueous medium are shown in Fig. 3. As can be seen from this figure, the resistivity increases with a decrease in the temperature and has an activation character, which is typical of semiconductors. Figure 4 shows the same dependences for the NDC10.2 samples irradiated in a helium atmosphere.

Since the NDC composites have a high volume content of pores with sizes of approximately 10 nm, it is necessary to examine adsorption properties of the samples prior to irradiation. For this purpose, we investigated the effect of water on the temperature dependence of the resistivity. The measurements showed that, after treatment in water for a few days at

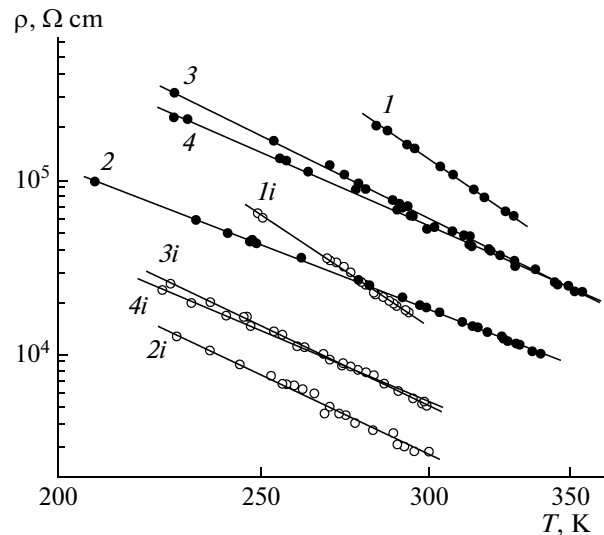


**Fig. 4.** Temperature dependences of the electrical resistivity of (1–4) the NDC10.2 samples irradiated with fluences  $F = (1) 5 \times 10^{17}$ , (2)  $1 \times 10^{18}$ , (3)  $2 \times 10^{18}$ , (4)  $5 \times 10^{18} \text{ cm}^{-2}$  and (1i–4i) the same samples before irradiation.

a temperature of 80°C, the resistivity increased several times.

As is known, the adsorption changes the filling of surface levels with electrons and acts like an external electric field [5]. The levels can be of both the acceptor type and the donor type with a concentration of  $10^{11}$ – $10^{12} \text{ cm}^{-2}$ . This circumstance should be taken into account when irradiation of samples is performed in reactor channels filled with water.

Fast neutron irradiation was carried out in vertical channels of the WWR-M reactor at the Konstantinov Petersburg Nuclear Physics Institute ( $E > 0.5 \text{ MeV}$ ). For filtering of thermal neutrons generating impurities due to transmutation, the samples were placed in a 0.5-mm-thick cadmium cover and in an aluminum container with holes for cooling with water. In order to eliminate the heating caused by the  $\gamma$ -ray absorption, the irradiation of the samples in the reactor was carried out in an aqueous medium of experimental channels at a temperature of  $\sim 50^\circ\text{C}$ . The samples NDC10.1 and NDC40 were irradiated in an aqueous medium, whereas the NDC10.2 samples were irradiated in quartz ampoules with helium, which were free of the aqueous medium. The irradiation was performed with fast neutron fluences in the range from  $5 \times 10^{16} \text{ cm}^{-2}$  to  $5 \times 10^{18} \text{ cm}^{-2}$ . The error in the determination of the fluence was 20%.

Figures 3 and 4 show the temperature dependences of the electrical resistivity of the NDC10 samples after irradiation with different fluences of fast neutrons in an aqueous medium and in quartz ampoules filled with helium. As can be seen from these figures, the resistivity of the NDC10 samples after irradiation nonmono-

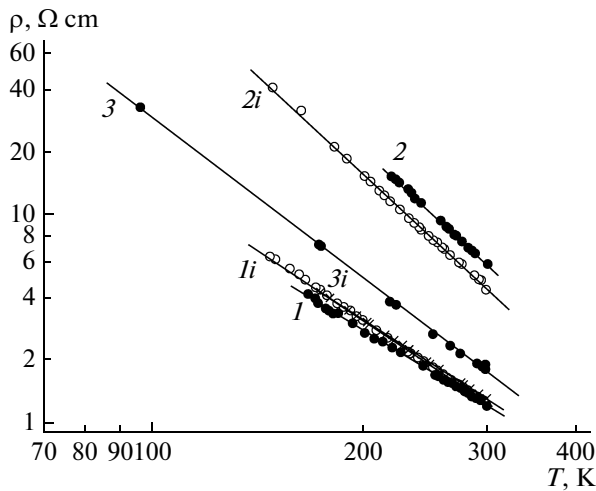


**Fig. 5.** Temperature dependences of the electrical resistivity of (1–3) the NDC40 samples irradiated with fluences  $F = (1) 1 \times 10^{17}$ , (2)  $1 \times 10^{18}$ , and (3)  $5 \times 10^{18} \text{ cm}^{-2}$  and (1i–3i) the same samples before irradiation.

tonically varies with an increase in the neutron fluence.

The electrical resistivity of the NDC40 samples is significantly less than that of the NDC10 samples (Fig. 5), because the thickness of the conductive pyrolytic carbon layer in NDC40 is four times larger than that in NDC10 (see table). The NDC40 samples were irradiated only in an aqueous medium. It is important that, as in the NDC10 samples, the resistivity of the NDC40 samples varies nonmonotonically with an increase in the neutron fluence.

In order to analyze the nonmonotonic change in the resistivity with an increase in the neutron fluence, we plotted the dependences of the relative change in the resistivity at different measurement temperatures on the neutron fluence. The dependences plotted in these coordinates allow one to elucidate the regularities of the variation in the resistivity by minimizing the effect of the significant spread in properties of the studied samples.

Figure 6 shows the relative change in the electrical resistivity at 300 K ( $\Delta\rho/\rho$ ) as a function of the neutron fluence for NDC10.1 (Fig. 6a) and NDC40 (Fig. 6c) irradiated in an aqueous medium and for NDC10.2 (Fig. 6b) irradiated in ampoules with helium. In these plots, we indicate the error in the measurement of the relative resistivity due to the technological spread in properties of the studied samples. The dependences of the resistivity on the neutron fluence have a complex nonmonotonic behavior. Usually, in the case of irradiation of various materials (metals, semiconductors, insulators, etc.), an increase in the neutron fluence leads to degradation of the main properties of the material, in particular, to an increase in the resistivity

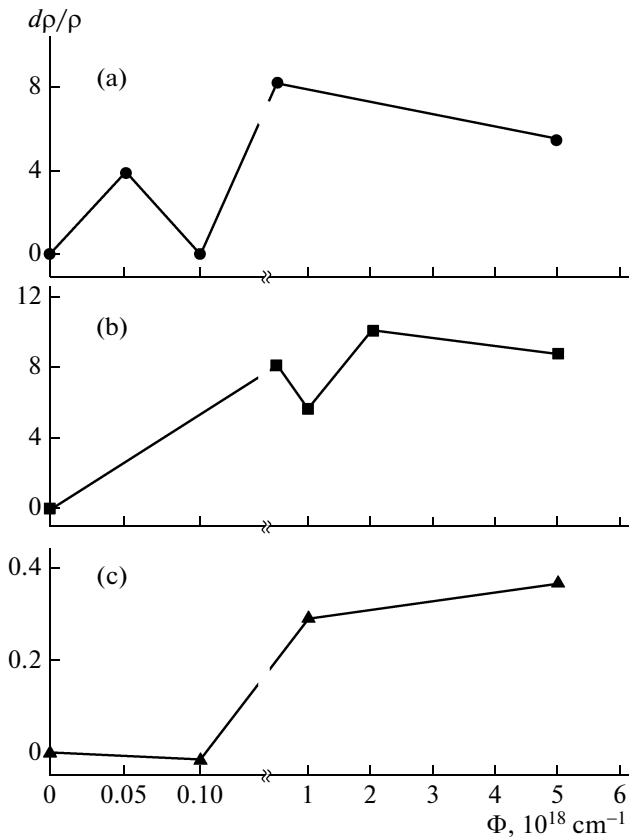


**Fig. 6.** Relative change in the electrical resistivity of the NDC samples as a function of the fast neutron fluence at 300 K: (a) NDC10.1, (b) NDC10.2, and (c) NDC40.

due to the generation of radiation defects and the increase in the degree of disorder.

As can be seen from Figs. 6a and 6b, the electrical resistivity of the NDC10 samples in the initial irradiation stages increases, then decreases to almost the initial values (NDC10.1), after which again begins to increase and, at fluences above  $10^{18} \text{ cm}^{-2}$ , remains almost unchanged. For the NDC40 samples irradiated in an aqueous medium (Fig. 6c), there is no region of the initial increase in the resistivity, which is observed for the NDC10 samples. The resistivity remains almost unchanged to the neutron fluence of  $1 \times 10^{17} \text{ cm}^{-2}$ . Then, the resistivity sharply increases to the fluence of  $1 \times 10^{18} \text{ cm}^{-2}$  and then smoothly varies to the neutron fluence of  $1 \times 10^{19} \text{ cm}^{-2}$ .

### 3. DISCUSSION OF THE RESULTS

For the explanation of the unusual change in the electrical resistivity with an increase in the neutron fluence, it is necessary to understand the character of changes in temperature dependences of the resistivity before and after the neutron irradiation. It should be noted that, at present, there are no generally accepted

physical concepts of the mechanisms responsible for charge transfer in carbon–carbon nanocomposites.

As was noted above, in the NDC composite, there are three types of interrelated compatible nanofragments, namely, nanodiamonds, a nanoscale graphite-like matrix (pyrolytic carbon), and nanopores. The conductive pyrolytic carbon matrix has a quasi-two-dimensional graphite-like structure, in which the majority of the carbon atoms reside in the  $sp^2$ -hybridized state and the conductivity has an activation character [6–11]. The pyrolytic carbon phase partially fills the space between nanodiamond particles, and the conduction can be provided by tunneling through the potential barriers over the localized states near the surface of particles [11]. It can be assumed that the total conductivity of this system should have a power-law dependence on the temperature, which will be determined by the average number of localized states [12].

In a number of studies [11–14], it was shown that, in materials with a quasi-two-dimensional graphite structure—this structure is observed in the pyrolytic carbon phase of the NDC samples—the temperature dependence of the conductivity can be explained in the framework of the two-dimensional graphite band model, which takes into account the smearing of the density of states due to non-thermal electron scattering by in-layer defects. In our case, the presented experimental data on the temperature dependence of the resistivity of the samples NDC10 and NDC40 (Figs. 3–5) before and after irradiation are best approximated by the power-law relationship

$$\rho(T) \sim \exp(-C/T)^{1/n} \quad (1)$$

with the parameter  $n = 4$ .

As is known, the dependence described by relationship (1) is characteristic of variable-range hopping conduction in the case of the so-called strong localization in systems with semiconductor conductivity in the presence of a local disorder [10]. At high temperatures ( $T > 100$  K), the temperature dependence of the hopping conductivity with  $n = 3$  was observed in [9], where it was attributed to two-dimensional localization in graphite-like systems, when a significant contribution to the charge carrier concentration is made by extrinsic charge carriers associated with defects in graphite layers. At low temperatures close to liquid-helium temperatures ( $T < 20$  K), the obtained value  $n = 2$  indicates a dominant role of the Coulomb gap [13, 15]. In the general case, the coefficient in expression (1) can vary from 2 to 4 depending on the dimensionality of charge carrier motion and on whether or not the Coulomb gap exists in the system [13]. It can be assumed that the conductivity of carbon–carbon composites should be determined by the corrections related to the mechanism of two-dimensional weak localization [10, 13].

In [12], it was assumed that the changeover from the linear dependence to the power-law dependence

of the conductivity of carbon composites on the temperature is associated with the influence of transitions between the dangling and deformed graphene layers in the composite with a complex microstructure. It is also assumed that the structure of pyrolytic carbon around the nanodiamonds in the NDC composite is similar to the structure of curved graphene upon high-temperature conversion of nanodiamonds into “onion-like” structures [11, 16, 17].

It is known that the interaction of radiation with a solid leads to the formation of structural defects of different types in the lattice. The character of structural distortions and their influence on the electrophysical properties of the irradiated material are determined by the lattice structure as well as by the nature and energy of the bombarding particles. Depending on the energy transferred to a lattice atom by an incident particle, there can arise two types of defects. If the energy transferred to the lattice atom by the incident particle is slightly higher than the threshold energy  $E_d$ , there arise simple isolated Frenkel defects (vacancies and interstitial atoms) and their complexes with impurity atoms. In the case where the energy of particles is high enough ( $E \gg E_d$ ), the initially displaced atom is able to create a cascade of displacements.

The state of a substance due to the energy transfer can be represented as an instantaneous ( $\approx 10^{-12}$  s) heating of a bounded region of the lattice to temperatures above the melting point [18, 19]. In this case, there arise regions with sizes of  $\sim 10$  nm, which contain approximately  $10^3$ – $10^4$  atoms in the form of displacement wedges, dislocations, or disordered regions of spherical shape [20]. As was shown in [20], such disordered regions in semiconductors reach sizes of approximately 10 nm; i.e., they cover several tens of interatomic distances. A similar pattern should be observed in the NDC samples, both in the nanodiamond particles and in the graphite-like pyrolytic carbon matrix, whose sizes are smaller than those of disordered regions created by neutrons. Thus, the fast neutron irradiation should lead to a very strong disorder of all carbon phases of the composite.

Reasoning from the schematic drawing of the material structure shown in Fig. 1, it can be assumed that the change in the resistivity of the material is associated with two transformation processes: the diamond–graphite phase transition or structural order–disorder transformations occurring in the graphite-like matrix. Moreover, the increase in the resistivity can be related to a partial transformation of the graphite-like matrix into diamond. This is possible if we take into account that, because of the small thickness of the graphite-like matrix in the considered materials, even the transformation of a fraction of its monolayer into diamond will lead to a significant increase in the resistivity. As was noted previously, nanodiamonds with sizes of 4–6 nm are thermodynamically more stable than graphites of the same sizes. Therefore, the struc-

tural transformation of a part of the graphite-like matrix layer adjacent to the surface of the nanodiamond particle into the diamond structure is quite possible. It should be noted that, from the chemical point of view, the graphite–diamond transition is reduced to a change in the character of the hybridization of the carbon atom and to its embedding in the tetrahedral environment.

It is possible that, during graphitization of nanodiamonds due to significant differences in molar volumes of carbon in these structures under irradiation with fast neutrons, no radical change in the overall structure of the material will occur.

By analyzing the above considerations and results, we can assume that, under irradiation of the NDC composite with low neutron fluences, the graphite-like component of the material apparently undergoes ordering. An increase in the neutron fluence leads to a partial transformation of the graphite-like matrix into diamond, which proceeds at the boundary of these phases. The fact that the process of diamond formation occurs after the ordering of the structure of the graphite-like matrix follows from the known results on the synthesis of diamonds at high pressure and high temperature, because the use of crystalline graphites is more preferable and makes it possible to soften conditions of diamond formation (to decrease the pressure and temperature). It can be expected that, in the considered case, too, the formation of diamonds will occur after the ordering of the structure of the graphite-like matrix of the material.

Along with these circumstances, the complex picture of the observed change in the resistivity with an increase in the neutron fluence due to the NDC multiphase nanostructure is predominantly determined by surface states in each nanophase in accordance with the theoretical concepts developed in the works by Tamm [21] and, later, Lifshitz and Pekar [22] on the one-dimensional and two-dimensional bands of surface electronic states in diamond.

It can also be assumed that, during neutron irradiation, when all phases of the nanocomposite undergo local heating to melting temperatures, the peeling of graphene sheets from the diamond core (“onion”) is possible [11, 23, 24]. However, all the proposed explanations have a purely qualitative character and, obviously, do not exhaust the complex processes occurring in the NDC nanocomposite.

#### 4. CONCLUSIONS

The performed investigations revealed that the temperature dependence of the electrical resistivity of the NDC nanocomposite is described by the exponential function with an exponent of 1/4 as for the unirradiated samples and the samples irradiated with fast neutrons in an argon atmosphere or in an aqueous

medium. With an increase in the neutron fluence, the resistivity changes nonmonotonically.

The unambiguous explanation of the obtained results is very difficult because there has been offered no generally accepted model that fully describes charge transfer in structures based on nanodiamonds. It can be assumed that, under neutron irradiation, there occurs a “pyrolytic carbon–diamond” transformation at the interface between these structural components. However, we cannot exclude the possibility of the reverse transition. It is also obvious that the neutron irradiation strongly disturbs the surface of diamond particles due to the continuous generation of point defects and their migration toward the surface. In this case, the spectrum of Tamm surface states changes, which can lead to a change in the electrical transport properties. Details of these processes remain unclear, and further experimental and theoretical studies are required to fully understand the nature of the electrophysical properties of the NDC nanocomposite and their dependence on the radiation exposure.

#### ACKNOWLEDGMENTS

This study was supported by the Ministry of Education and Science of the Russian Federation (state contract nos. 14.518.11.7028 and 16.518.11.7034) and the Russian Foundation for Basic Research (project no. 10-02-00576).

#### REFERENCES

1. V. V. Danilenko, *Diamond Synthesis and Sintering by Explosion* (Energoatomizdat, Moscow, 2003) [in Russian].
2. S. K. Gordeev, *Sverkhtverd. Mater.* **6**, 60 (2002).
3. S. K. Gordeev, P. I. Belobrov, N. I. Kiselev, E. A. Petravskaya, and T. C. Ekstrom, *Mater. Res. Soc. Symp. Proc.* **638**, F14.16.1 (2001).
4. I. V. Golosovsky, I. Mirebeau, E. Elkaim, D. A. Kurdyukov, and Yu. A. Kumzerov, *Eur. Phys. J. B* **47**, 55 (2005).
5. E. I. Grigor'ev, P. S. Vorontsov, S. A. Zav'yalov, and S. N. Chvalun, *Tech. Phys. Lett.* **28** (10), 845 (2002).
6. A. S. Kotosonov, *JETP Lett.* **43** (1), 37 (1986).
7. A. S. Kotosonov, *Sov. Phys. JETP* **66** (5), 1068 (1987).
8. A. S. Kotosonov, *Sov. Phys. Solid State* **33** (9), 1477 (1991).
9. A. S. Kotosonov, *Sov. Phys. Solid State* **31** (8), 1359 (1989).
10. L. V. Lutsev, T. K. Zvonareva, and V. M. Lebedev, *Tech. Phys. Lett.* **27**, (8), 659 (2001).
11. P. I. Belobrov, in *Proceedings of the 9th International Conference “High Technology in Russian Industry,” Central Research Technological Institute “Tekhnomash,” Moscow, September 11–13, 2003*, p. 235.

12. E. I. Zhmurikov, Preprint No. 18, IYaF SO RAN (Budker Institute of Nuclear Physics, Siberian Branch of the Russian Academy of Sciences, Novosibirsk, 2005).
13. B. I. Shklovskii and A. L. Efros, *Electronic Properties of Doped Semiconductors* (Nauka, Moscow, 1979; Springer-Verlag, Berlin, 1984).
14. A. I. Romanenko, O. B. Anikeeva, A. V. Okotrub, L. G. Bulusheva, V. L. Kuznetsov, Yu. V. Butenko, A. L. Chuvilin, S. Dong, and Y. Ni, *Phys. Solid State* **44** (3), 487 (2002).
15. A. G. Zabrodskii, *Sov. Phys. Semicond.* **11** (3), 345 (1977).
16. V. L. Kuznetsov, A. L. Chuvilin, Y. V. Butenko, I. Yu. Mal'kov, and V. M. Titov, *Chem. Phys. Lett.* **222**, 343 (1994).
17. F. Banhart, *Phys. Solid State* **44** (3), 399 (2002).
18. G. J. Dienes and G. H. Vineyard, *Radiation Effects in Solids* (Interscience, New York, 1957; Inostrannaya Literatura, Moscow, 1960).
19. M. W. Thompson, *Defects and Radiation Damage in Metals* (Cambridge University Press, Cambridge, 1969; Mir, Moscow, 1971).
20. R. F. Konopleva, V. L. Litvinov, and N. A. Ukhin, *The Features of Radiation Damage of Semiconductors by High-Energy Particles* (Atomizdat, Moscow, 1971) [in Russian].
21. I. Tamm, *Z. Phys.* **76** (11–12), 849 (1932).
22. I. M. Lifshitz and S. M. Pekar, *Usp. Fiz. Nauk* **56** (4), 531 (1955).
23. A. S. Krylov, N. P. Shestakov, S. B. Korchagina, S. S. Tsegel'nik, D. A. Znak, A. A. Latynina, I. A. Denisov, N. V. Volkov, S. K. Gordeev, and P. I. Belobrov, in *Proceedings of the 17th International Conference "High Technology in Russian Industry," Bauman Moscow State Technical University, Moscow, September 8–9, 2011*, p. 382.
24. N. I. Kiselev, D. A. Velikanov, S. B. Korchagina, E. A. Petrakovskaya, A. D. Vasil'ev, L. A. Solov'ev, D. A. Balaev, O. A. Bayukov, I. A. Denisov, S. S. Tsegel'nik, E. V. Eremin, D. A. Znak, K. A. Shaikhutdinov, A. A. Shubin, N. P. Shestakov, N. V. Volkov, S. K. Gordeev, and P. I. Belobrov, *Russ. Khim. Zh.* **LVI** (1–2), 50 (2012).

*Translated by O. Borovik-Romanova*